Articles relacionats amb el Subcapítol 2.2

Article H

Títol: A nanoporous molecular magnet with reversible solvent-induced mechanical and magnetic properties.

Autors: D. Maspoch, D. Ruiz-Molina, K. Wurst, N. Domingo, M. Cavallini, F. Biscarini, J. Tejada, C. Rovira, J. Veciana.

Publicació: Nature Mat. 2003, 2, 190.

A nanoporous molecular magnet with reversible solvent-induced mechanical and magnetic properties

DANIEL MASPOCH[1], DANIEL RUIZ-MOLINA[1], KLAUS WURST[2], NEUS DOMINGO[3], MASSIMILLIANO CAVALLINI[4], FABIO BISCARINI[4], JAVIER TEJADA[3], CONCEPCIÓ ROVIRA[1] AND JAUME VECIANA*[1]

[1]Institut de Ciència de Materials de Barcelona (CSIC), Campus Universitari de Bellaterra, 08193-Cerdanyola, Spain
[2]Institut für Allgemeine, Anorganische und Theoretische Chemie, Universität Innsbruck, Innrain 52a, A-6020 Innsbruck, Austria
[3]Facultad de Física, Universitat de Barcelona, Diagonal 647, 08028-Barcelona, Spain
[4]CNR-Istituto per lo Studio dei Materiali Nanostrutturati (CNR), Via P. Gobetti 101, I-40129-Bologna, Italy
*e-mail: vecianaj@icmab.es

Published online 16 February 2003; doi:10.1038/nmat834

Interest in metal–organic open-framework structures has increased enormously in the past few years because of the potential benefits of using crystal engineering techniques to yield nanoporous materials with predictable structures and interesting properties. Here we report a new efficient methodology for the preparation of metal–organic open-framework magnetic structures based on the use of a persistent organic free radical (PTMTC), functionalized with three carboxylic groups. Using this approach, we create an open-framework structure $Cu_3(PTMTC)_2(py)_6(CH_3CH_2OH)_2(H_2O)$, which we call MOROF-1, combining very large pores (2.8–3.1 nm) with bulk magnetic ordering. MOROF-1 shows a reversible and highly selective solvent-induced 'shrinking–breathing' process involving large volume changes (25–35%) that strongly influence the magnetic properties of the material. This magnetic sponge-like behaviour could be the first stage of a new route towards magnetic solvent sensors.

The exceptional characteristics of nanoporous materials have prompted their technological applications in different fields such as molecular sieves, sensors, ion-exchangers and catalysis. In this context, zeolites and metal phosphates have been the predominant class of porous solids used so far[1]. However, in the past few years, the use of polyfunctional organic linkers has become an attractive alternative strategy for achieving new metal–organic open frameworks[2–4]. The assembly of metal ions with several types of polytopic organic linkers[5–8] has yielded a large variety of extended porous frameworks with a considerable range of pore sizes and functionalities. Furthermore, the construction of open frameworks from transition metal ions opens the possibility of designing functional nanoporous materials with additional physical properties. Among these, the search for magnetic open-framework structures using diamagnetic polyfunctional carboxylic acids is a great challenge[9–13]. One new nanoporous metal coordination polymer[14] uses the 1,3,5-benzenetricarboxylic acid (BTC), which has a three-dimensional structure with a pore size of 9 Å and a cooperative antiferromagnetic behaviour. A more recent example has a Kagomé-like open framework with microscopic pores (9 Å) and a spin-canting effect[15].

But there are enormous difficulties in expanding pore sizes without compromising the strength of magnetic exchange interactions. Indeed, magnetic coupling between transition metal ions takes place through a superexchange mechanism involving ligand orbitals, a mechanism that is strongly dependent on their relative orientation and especially on the distance between interacting ions. Although a systematic approach has been described for the design of pore size and functionality based on the use of organic polyfunctional diamagnetic carboxylate ligands with different lengths and topologies[16,17], such modifications are expected to decrease, or in the worst case disrupt, the superexchange pathway. To overcome this inconvenience, alternative methodologies are being developed[9,18]. Examples are molecular magnets based on hybrid organic–inorganic structures with long-range ferromagnetism; these

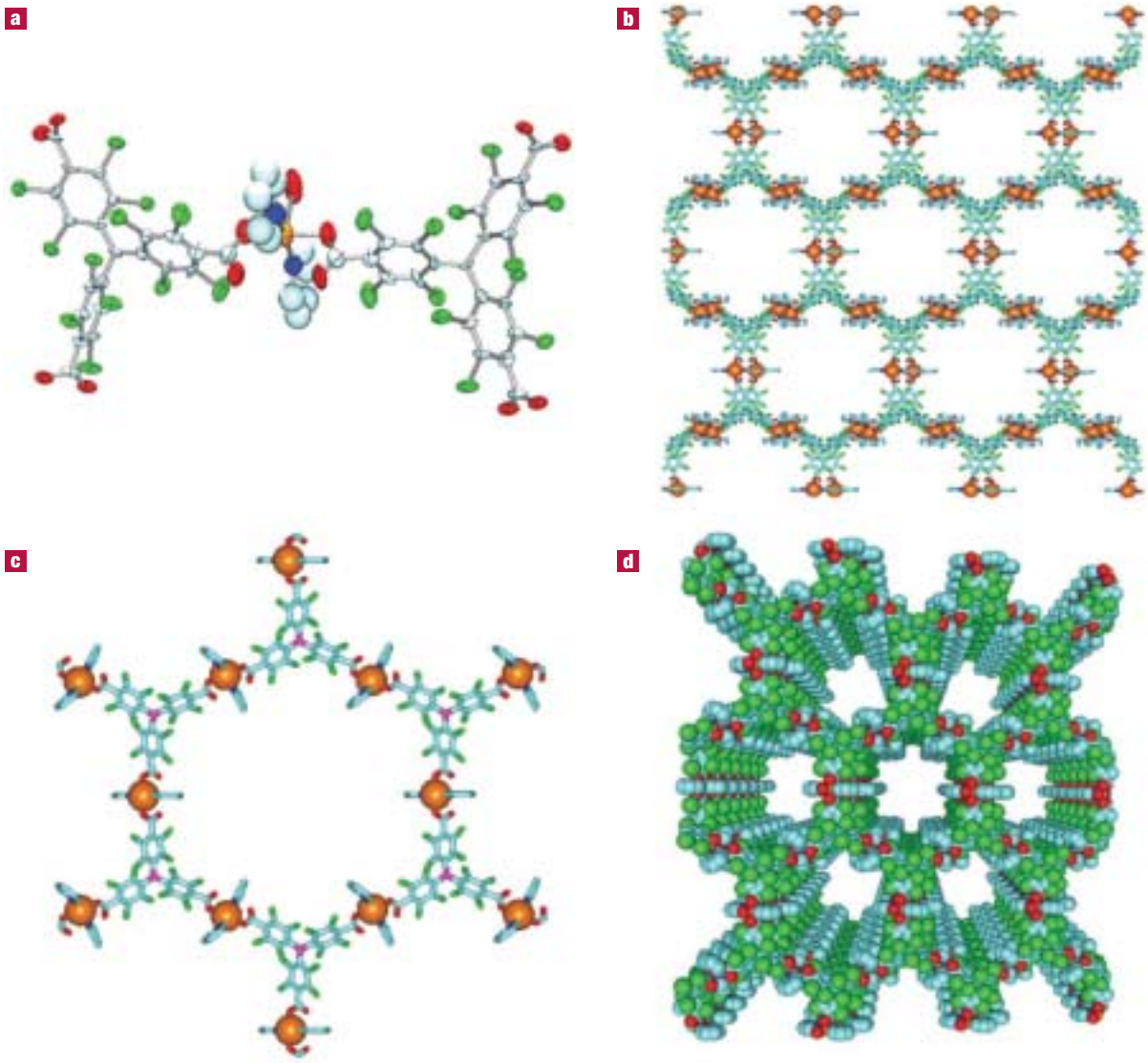

Figure 1 Crystal structure of MOROF-1. The structure has the formula $Cu_3(PTMTC)_2(py)_6(CH_3CH_2OH)_2(H_2O)$ **a**, ORTEP (Oak Ridge thermal ellipsoid plot) of copper(II) tricarboxylate building block. **b**, Honeycomb arrangement of layers in an ABAB disposition along the *a*–*b* plane. The minimum distance between Cu(II) ions of neighbouring layers is 8.53 Å. **c**, Hexagonal pores: the carbon atoms depicted in violet, which have most of the spin density of PTMTC radicals, are located in the vertices of hexagons. Cu(II), depicted in orange, are located in the middle of hexagon sides. **d**, A view in the [001] direction, showing the distribution of the nanopores of the open framework. Cu, orange; C, light blue; O, red; Cl, green; and N, dark blue. Guests and hydrogen atoms are omitted for clarity.

materials are potentially porous, depending on the distance between the layers[19].

Here we present a new, efficient and reliable synthetic strategy for obtaining metal–organic open-framework materials with very large pores and relatively strong magnetic exchange interactions that become ordered at low temperature. Our approach is based on the combination of magnetically active transition metal ions with persistent polyfunctionalized organic radicals as polytopic ligands. The open-shell character of organic radical ligands is particularly appealing because they are expected to interact magnetically with transition metal ions, increasing the magnetic interactions of the nanoporous material. Therefore, metal–organic radical open-frameworks (MOROF) structures are expected to have larger magnetic couplings and dimensionalities than systems made up of diamagnetic polyfunctional coordinating ligands. For this synthetic approach we chose polychlorinated triphenylmethyl (PTM) radicals, in which the central carbon atom, where most of the spin density is localized, is sterically shielded by six bulky chlorine atoms. This encapsulation produces a remarkable increase in the lifetime and thermal and chemical stability of the radical[20]. We used as our polytopic ligand a PTM radical functionalized with three carboxylic groups (TC) at the *para* position of phenyl rings with respect to the central carbon (D. Maspoch, D. Ruiz-Molina, C. Rovira and J. Veciana, manuscript in preparation). The conjugated base of this PTMTC radical can be considered an expanded version of the BTC^{3-} ligand, where the benzene-1,3,5-triyl unit has been replaced by an sp^2 hybridized carbon atom decorated with three 4-substituted 2,3,5,6-tetrachlorophenyl rings. Therefore, given their related trigonal symmetries and functionalities, $PTMTC^{3-}$ is also expected to yield open-framework structures similar to those of BTC^{3-} but with larger pore sizes.

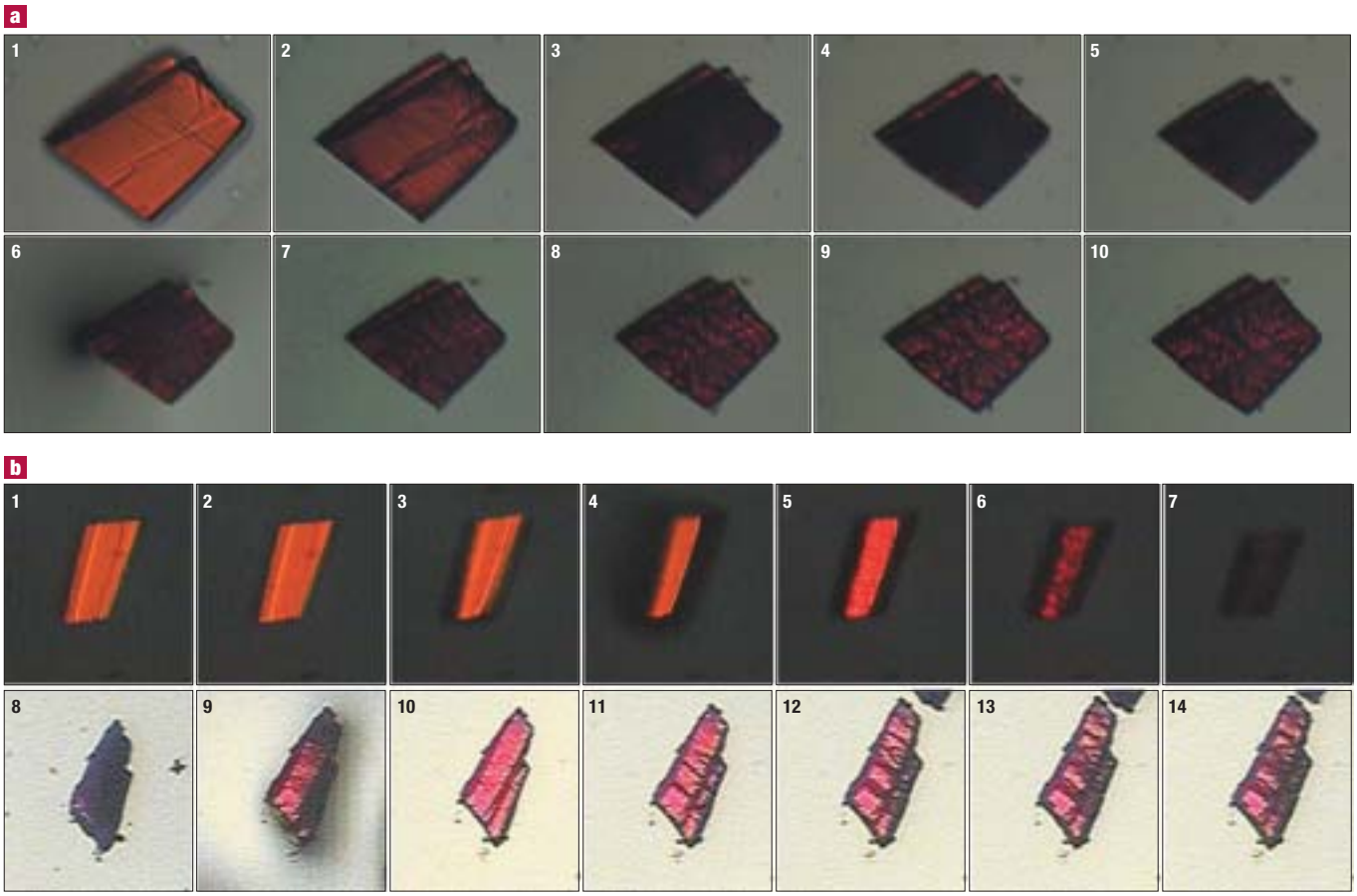

Figure 2 Real images of crystals of MOROF-1 followed with an optical microscope. a, Initially, the crystal was in contact with ethanol solvent. The top series of images (1–5) were taken at 0, 2, 8, 15 and 40 seconds after the crystal was removed. In (1) ethanol solvent, which moistens the crystal, is partially evaporated; in (2), after only 2 s, solvent is completely evaporated and the crystal begins to reduce rapidly in volume, becoming dark. A drop of ethanol was then placed on the crystal, and the lower series of images (6–10) were taken at 0, 2, 6, 14 and 25 s. **b**, Crystal changes viewed under polarized light. Upper series of images (1–7) were taken at 0, 1, 3, 5, 8, 14 and 20 s after the exterior solvent had completely evaporated. The crystal begins to contract and darken within seconds. In the lower series of images, image 8 shows a different amorphous dark crystal in contact with air atmosphere. In 9, at 0 s, a drop of ethanol was placed on the crystal. Immediately we begin to recover the brightness. Images 10–14 were taken at 2, 10, 20, 40 and 60 s after this.

In the reaction, an ethanol solution (20 ml) containing pyridine (3 ml) was layered onto a solution of $Cu(ClO_4)_2{\cdot}6H_2O$ (0.053 g, 0.143 mmol) and PTMTC radical (0.075 g, 0.095 mmol) in ethanol (15 ml) and water (5 ml). Slow diffusion over 14 days yielded red needle crystals of $Cu_3(PTMTC)_2(py)_6(CH_3CH_2OH)_2(H_2O)$ (referred to as MOROF-1). The MOROF-1 complex is completely insoluble in water and most common organic solvents. Single-crystal structure analysis revealed that the electrically neutral polymer framework of MOROF-1 is composed of Cu^{2+} units with a square pyramidal coordination polyhedron formed by two monodentate carboxylic groups and two pyridine ligands (see Fig. 1). The remaining positions on the coordination sites of the metal centres are occupied by coordinative solvent molecules of ethanol or water, in a relationship of 2:1, as occurs in a related Cu^{2+} complex[21]. Moreover, because each Cu^{2+} ion is coordinated to two neighbouring $PTMTC^{3-}$ ions and each $PTMTC^{3-}$ binds to three Cu^{2+} units, the stoichiometry of the network is Cu^{2+}:$PTMTC^{3-}$ = 3:2, which generates a two-dimensional layer extending along the *a*–*b* plane with a honeycomb structure. Simultaneously, different layers arrange themselves between them, by means of weak π···π and van der Waals interactions, forming an open-framework structure (Fig. 1). A view along the [001] direction of the monoclinic cell of MOROF-1 reveals the presence of hexagonal nanopores, each composed of a ring of six metal units and six PTMTC radicals, which measure 3.1 and 2.8 nm between opposite vertices. To our knowledge, these are some of the largest nanopores yet reported for a metal–organic open-framework structure[22,23]. Moreover, the MOROF-1 complex shows square and rectangular channels in the [100] direction with estimated sizes of 0.5 × 0.5 and 0.7 × 0.3 nm, respectively. The larger pores in the [001] direction together with those pores in the [100] direction produce solvent-accessible voids in the crystal structure that amount to 65% of the total unit cell volume (21,805 $Å^3$). Therefore, in addition to the two coordinating solvent molecules of ethanol and one of water, X-ray analysis revealed additional ten guest molecules of ethanol and six of water per formula unit, hydrogen-bonded with the inner-walls of the pores. Further disordered guest molecules that could not be located in the crystal structure analysis fill the inner pore channels.

Single crystals of MOROF-1 removed from the solution lost solvent molecules very rapidly at room temperature, becoming an amorphous material, which recovered its structural integrity when re-immersed in liquid ethanol, as confirmed by X-ray powder diffraction (XRPD) patterns. Indeed, thermogravimetry/mass spectroscopy (TG-MS) analysis for the amorphous MOROF-1 confirmed that it does not contain any ethanol and water solvent molecules in its structure.

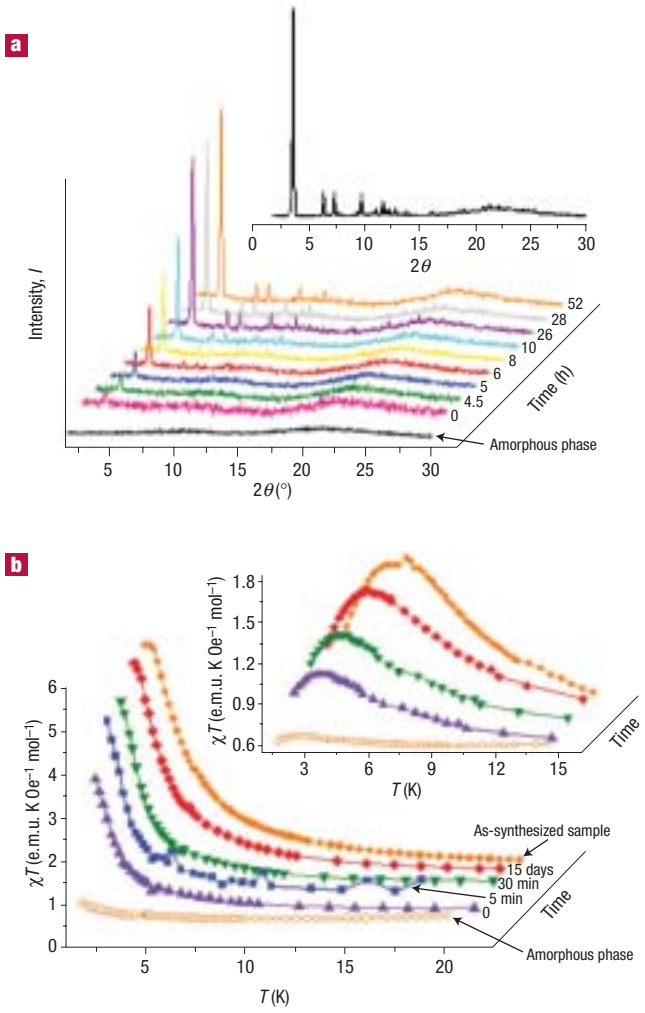

Figure 3 Guest exchange studies followed by magnetic and XRPD measurements. **a**, Powder X-ray diffractograms of MOROF-1, showing the steps of transformation of the amorphous, evacuated phase in contact with ethanol vapours. Inset: powder X-ray pattern of as-synthesized sample of MOROF-1. **b**, Reversible magnetic behaviour of the amorphous and evacuated phase in contact with ethanol liquid, as observed by plotting χT as a function of temperature T at a field of 1,000 Oe. Inset: similar behaviour at 10,000 Oe.

Thus, all solvent molecules including those coordinating the Cu^{2+} ion are completely lost at room temperature. Our interest in compound MOROF-1 increased after noticing the large and reversible structural transformations that follow the loss and retrieval of solvent molecules. As shown in Fig. 2a, a few single crystals of MOROF-1 were removed from the solution and their time evolution in air at room temperature was followed with an optical microscope. After a few seconds, a rapid volume contraction of the crystals was observed, the contraction being completely stabilized after 1 minute with a total volume reduction of 25–35%. Even more interesting, the contracted sample of MOROF-1 experiences a mechanical transformation, recovering up to 90% of their original size after exposure to liquid ethanol. Solvent-induced expansion/contraction processes in open-framework metal–organic polymers have been very recently reported[24–26], although the large volume changes shown by MOROF-1 (25–35%) have not been seen before. Similar time-dependent experiments followed with polarized light confirmed that the solvent-induced mechanical 'shrinking–breathing' process is accompanied by a gradual loss and recovery of crystallinity (Fig. 2b).

To give more insight into this unprecedented guest exchange phenomenon, an evacuated sample of MOROF-1, which did not show any XRD pattern, was exposed to ethanol vapour (or liquid) and allowed to stand for few days at room temperature, during which period we measured the powder XRD patterns (see Fig. 3a) and the magnetic susceptibility (χ) and its temperature (T) dependence (see Fig. 3b) at different intervals of time. The XRD patterns show an increase of crystallinity with time, which tends to stabilize after a few hours. The observed patterns are essentially identical to those observed for a few single crystals of an as-synthesized MOROF-1 sample in contact with the mother liquor, indicating a large degree of reversibility for the solvent-induced mechanical 'shrinking–breathing' process'. The solvent-induced structural changes are clearly reflected in the magnetic properties of the sample, as shown in Fig. 3b, confirming the reversibility of the guest exchange phenomenon.

In addition to ethanol solutions, evacuated MOROF-1 samples were also exposed to water and to a representative range of organic solvents, such as hexane, dichloromethane, benzene, chlorobenzene, toluene, tetrahydrofurane, acetonitrile, methanol, isopropanol, 1-propanol, 1,2-ethandiol, 1,2-propandiol, 2-propen-1-ol, 1-octanol and benzylic alcohol. Interestingly, MOROF-1 shows a high selectivity, only regenerating its framework and crystallinity after exposure to ethanol and methanol. This parallels the selectivity towards alcohols observed in another open-framework complex, which does not, however, show a complete loss of crystallinity on solvent evacuation[27].

We measured the magnetic properties of as-synthesized crystals of MOROF-1 in contact with ethanol. Plots of the product of the magnetic susceptibility and temperature (χT) as a function of temperature are shown in Fig. 4. At room temperature, the value of χT is equal to 1.8 e.m.u. K mol^{-1}. As the temperature is lowered, χT remains constant down to about 250 K, whereupon it decreases smoothly, reaching a minimum value at 31 K. Then, as temperature is further decreased, the χT curve increases very rapidly up to a maximum value around 2 K.

The χT value of 1.8 e.m.u. K mol^{-1} at room temperature is in good agreement with that expected for non-interacting Cu^{2+} ions and $PTMTC^{3-}$ radicals, with a 3:2 stoichiometry and local spins $S(Cu^{2+}) = S(PTMTC^{3-}) = ½$. The smooth decrease of the χT value below 250 K, arising from a depopulation of the high-spin excited states of the irregular spin-state structure of this complex, is a clear signature of the presence of an antiferromagnetic coupling between nearest-neighbouring Cu^{2+} and $PTMTC^{3-}$ ions within the honeycomb layers. In this case, the minimum of χT corresponds to a state with short-range order where the spins of adjacent magnetic centres are antiparallel, provided there is not a net compensation due to the 3:2 stoichiometry of the Cu(II) ions and $PTMTC^{3-}$ radical units. This spin system can be considered as a new two-dimensional system composed of two different quantum spins that show antiferromagnetic interactions with a particular hexagonal topology for whose magnetic behaviour there is still no theoretical model. Nevertheless, the strength of the effective antiferromagnetic exchange coupling between Cu(II) ions and $PTMTC^{3-}$ radical units has already been modelled and studied in a related discrete monomeric complex, formed by one Cu(II) ion and two PTM radicals functionalized with one carboxylate group, whose structure around the coordination sphere of Cu(II) is similar to MOROF-1. For this discrete radical complex a magnetic exchange coupling between the two radical units and the metal of $J/k_B = -22$ K was found (where J is the magnetic exchange coupling constant and k_B is the Boltzmann constant; see Supplementary Information)[28]. However, to give more insight into the origin of the antiferromagnetic interactions within the two-dimensional honeycomb layer, we obtained an isostructural complex to MOROF-1, where the open-shell ligand $PTMTC^{3-}$ has been replaced by its non-radical hydrocarbon counterpart (MOOF-1; see Methods), and studied its magnetic properties. Whereas the χT value of an as-synthesized sample of MOROF-1 decreases smoothly below 250 K, the χT plot of the

isostructural non-radical counterpart MOOF-1 shows quasi-ideal paramagnetic behaviour down to very low temperatures (see Supplementary Information). This result confirms the importance of using an open-shell ligand to enhance the strength of magnetic interactions within the metal–organic open framework, as the magnetic exchange interaction between Cu(II) ions through a superexchange mechanism within this diamagnetic ligand is negligible.

The low-temperature data suggest that MOROF-1 shows long-range magnetic ordering. Indeed, the huge increase of χT at low temperatures can be explained by an increase of the correlation length of antiferromagnetically coupled units of Cu^{2+} and $PTMTC^{3-}$ as randomizing thermal effects are reduced, either through in-plane long-range antiferromagnetic coupling or through interplane magnetic interactions. The latter are probably originated by dipolar–dipolar magnetic interactions between the large magnetic moments developed on the neighbouring layers at these temperatures, as occurs for many low-dimensional molecular systems[29–32]. Moreover, the value of χT shows a considerable dependence on the applied external magnetic field, as shown in Fig. 4b. Such a behaviour, saturation effects aside, is also characteristic of two-dimensional bimetallic complexes with oxalate bridges that show long-range magnetic ordering at low temperatures[29].

Magnetic properties of an evacuated amorphous sample of MOROF-1 were also measured. Remarkably, the temperature dependence of χT is similar to that of as-synthesized crystals of MOROF-1 (see Fig. 4a). This fact confirms that even though the volume of the sample can be reduced by up to 30%, the nature of the magnetic interactions—antiferromagnetic coupling—does not change. Two main points, however, deserve mention: first, from the distinct positions of the χT minima for as-synthesized and evacuated MOROF-1 samples (31 K and 11 K, respectively), it can be inferred that the effective strength of the interactions depends on the presence or absence of included solvent molecules. Such interactions decrease for the evacuated sample of MOROF-1, although the lack of its X-ray structure prevents us extracting any magneto-structural conclusion. Nevertheless, from a qualitative point of view, slight structural alterations around the coordination sphere of Cu(II) ions are expected to have a large influence on the magnetic exchange coupling[29]. Second, the magnetic response of the filled MOROF-1 sample at low temperature, where the long-range magnetic ordering is attained, is much larger (up to one order of magnitude) than that of the evacuated MOROF-1 material (see Figs 3b and 4a). Moreover, the maximum of the χT curve is shifted to lower temperatures, 400 mK, which is why a d.c.-SQUID placed in a dilution cryostat was used.

Further information on the three-dimensional magnetic ordering is provided by the a.c. magnetic responses and field dependence of the magnetization measurements (see Supplementary Information). We collected a.c. susceptibility measurements for an as-synthesized sample of MOROF-1, in contact with ethanol, between 1.8 and 10 K in a 1-G a.c. field oscillating at 3–100 Hz. Under these conditions, both the in-phase and out-of-phase a.c. magnetic susceptibilities present a maximum that depends very slightly on the frequency of the oscillating field. We also measured the field dependence of the magnetization at 2 K of evacuated crystals of MOROF-1 and of as-synthesized crystals (see Supplementary Information). In the latter case, the magnetization increases very rapidly for low external magnetic fields, as expected for a bulk magnet, then increases much more slowly at higher fields up to a saturation value of $1.2\mu_B$, close to that expected for a $S = {}^1/_2$ magnetic ground state. Interestingly, the field dependence of the magnetization at 2 K for as-synthesized MOROF-1 does not show any significant hysteresis, as occurs for molecular soft magnets[29,31]. This result is in accordance with the low magnetic anisotropic nature of Cu(II) ions and PTM radical units. On the other hand, the field dependence of the magnetization at 2 K of evacuated crystals of MOROF-1 shows a smooth increase up to an external field of 4 T, at which the saturation value is still not reached. The reason for such different behaviour is that,

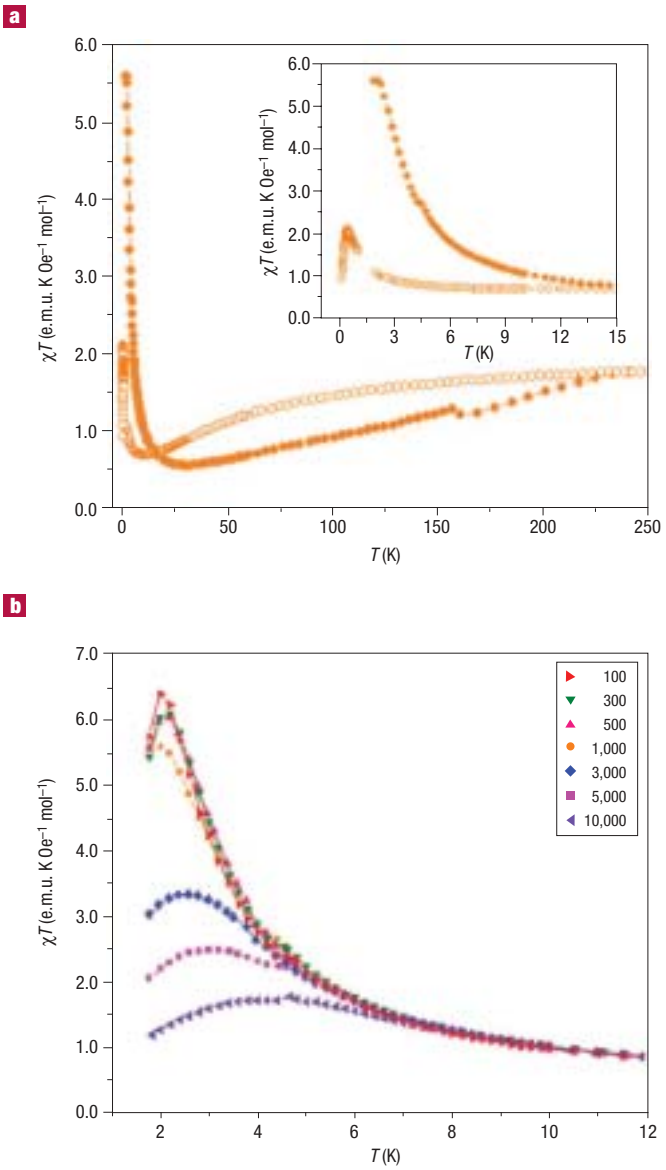

Figure 4 Magnetic properties. a, Value of χT as a function of the temperature for MOROF-1 (orange filled circle, MOROF-1; open circle, evacuated MOROF-1). The jump observed along this decay around 160 K, for the as-synthesized crystals in contact with ethanol, corresponds to the phase change of the solvent from liquid to glass. **b**, Value of χT as a function of temperature for filled MOROF-1 at different applied fields H(Oe).

whereas the as-synthesized sample of MOROF-1 shows long-range magnetic order below 2 K, the evacuated sample still behaves as a paramagnet in this temperature range.

Finally, the increased magnetic response of a filled sample compared with an evacuated sample of MOROF-1, together with the reversible solvent-induced structural changes in this sponge-like material, open the door to the possible development of magnetic sensors based on open-framework molecular magnets. The most striking point is that the structural evolution of the material during solvent inclusion can be completely monitored by the magnetic properties. Figure 3b shows the evolution of the χT curve with time, once an evacuated sample of MOROF-1 has been exposed to a solvent in either liquid or vapour phase (see also Supplementary Information for evolution of field dependence

of magnetization with time). A fast recovery up to 60% of the signal can be seen during the first minutes, after which the recovery of magnetic signal seems to be linear with the logarithm of time. Moreover, of more than 15 different solvents so far used, including several alcohols, the reversible behaviour has only been observed for ethanol and methanol, showing the selectivity of the sponge-like magnetic sensor.

METHODS

STRUCTURAL STUDIES

All the intensity data were collected on a Nonius KappaCCD diffractometer with a graphite monochromatic MoK$_\alpha$ (λ = 0.71073 Å) radiation. Each crystal of MOROF-1 was measured at room temperature in a glass capillary, which was partially filled with mother liquors. The diffraction images showed considerable background scattering (diffuse scattering) caused by the disordered molecules of water and ethanol in the channels of the crystal lattice. A Cu(py)$_2$(H$_2$O)-unit, lying in a special position (mirror plane), was 1:1 disordered into two positions connecting to the oxygen atoms O5 or O6. The pyridine rings show overlapping positions and could only be refined as rigid groups (fixed coordinates) with fixed and estimated thermal parameters. Crystal data are as follows: $C_{78}H_{44}Cl_{24}Cu_3N_6O_{15}\cdot 6H_2O\cdot 10C_2H_6O$, relative molecular mass M_r = 2,915.39, monoclinic crystal system, space group $C2/m$, a = 29.841(4) Å, b = 48.069(8) Å, c = 16.360(2) Å, β = 111.698(4)°, V = 21,804.5(54) Å^3, formula units per cell Z = 4, conventional discrepancy index R_1 = 0.0967 and weighted wR_2 = 0.2564, calculated with $I > 2\sigma(I)$. The structure was refined with SHELXL93. Single-crystal XRD data are available as Supplementary Information. The coordinates are on deposit with the Cambridge Structural Database, deposit number CCDC194815.

A non-radical analogue complex of MOROF-1 was obtained using the non-radical counterpart of PTMTC—a polychlorinated triphenylmethane derivative substituted with three carboxylic groups, HPTMTC—as the organic ligand under similar experimental conditions. This procedure yielded an isostructural complex with MOROF-1, Cu$_3$(HPTMTC)$_2$(py)$_6$(CH$_3$CH$_2$OH)$_2$(H$_2$O), named as MOOF-1 (space group $C2/m$, a = 29.843(1) Å, b = 48.40(1), c = 16.34(1), β = 110.87(3)°, V = 22,055(20) Å^3). Comparison of XRPD spectra of MOROF-1 and MOOF-1 is available as Supplementary Information.

Analysis of nanopore sizes of the MOROF-1 crystal structure was done with a commercial software package (CERIUS). Hexagonal nanopores measure 3.4 and 3.2 between opposite sites, and an effective size of 2.8 and 3.1 nm is obtained when van der Waals radii are considered. Taking into account the Cl atoms located at the walls of the hexagonal channels, the medium effective size of the cavities is estimated to be 2.5 × 2.3 nm. The distances between Cu(II) atoms of opposite sites of the pore are 3.1 and 2.8 nm. The closest contacts between opposite sites correspond to pyridine molecules with distances of 2.2 and 2.4 nm and effective size of 1.8 × 2.0 nm. The solvent accessible volume was calculated using the A.M.C.T. PLATON (A. L. Spek, Utrecht University, 1998).

THERMAL STUDIES

The thermal stability of MOROF-1 was studied with TG-MS. The results showed that a sample of MOROF-1 that had been evacuated at room temperature only lost mass at 453 K, which corresponded to the formation of CO_2 and few side-reaction decomposition products. No peaks attributable to the presence of ethanol or of water were observed, indicating that all solvent molecules have already been lost at room temperature. This result was in agreement with elemental analysis.

MICROSCOPY

The study of 'shrinking and breathing' of MOROF-1 crystals was done using an optical polarized microscope with an incorporated colour CCD camera (Panasonic Industrial, model GP-KR222E). Videos of the structural transformation of crystals of MOROF-1 are available as Supplementary Information. The mean volume contraction of MOROF-1 crystals was calculated from the external dimensions of several crystals as observed with the optical microscope. Because only two dimensions could be directly observed, the volume contraction was calculated by fixing the unobserved direction and giving it a minimum value of 25%. Along with the large volume contraction, several cracks were produced in the crystal. These fractures originated from the large stress occurring during the structural rearrangement, which cannot be released because of the lack of flexibility of the organic radical ligand within the open-framework structure.

X-RAY POWDER DIFFRACTION

Guest-exchange studies with MOROF-1 were followed by X-ray powder diffraction experiments with a diffractometer (INEL CPS-120) of Debye–Scherrer geometry. For this purpose, evacuated crystals of MOROF-1 were placed in a capillary and exposed to vapours of different solvents.

MAGNETIC MEASUREMENTS

Magnetic measurements were done with a commercial SQUID magnetometer (MPMS2) in the temperature range 1.8 to 300 K. For temperatures down to millikelvins, a d.c.-SQUID placed in a dilution cryostat was used. The MPMS2 magnetometer has sensitivity down to 10^{-7} e.m.u., a precision of 1 Oe for the applied magnetic field, and relative error in temperatures of less than $5^0/_{00}$. The evacuated MOROF-1 samples had a powdery appearance and were measured by placing the sample in a small hermetically sealed plastic bag. The filled MOROF-1 samples had to be kept in ethanol during measurements, so they were placed in a cylindrical Teflon container filled with ethanol, which was closed hermetically with a screw-on lid to prevent evaporation of the solvent due to the low pressure inside the sample chamber. The temperature and field dependence of the sample holder with ethanol were measured alone and data were subtracted from the results.

MOOF-1 complex shows a quasi-ideal paramagnetic behaviour down to 5 K with an effective magnetic moment of 2.8μ_B per formula unit (where μ_B are Bohr magnetons) which corresponds to the value expected for a system with three non-interacting Cu(II) ions ($S = {}^1/_2$) per formula unit.

Received 24 October 2002; accepted 16 January 2003; published 16 February 2003

References

1. Cheetham, A. K., Férey, G. & Loiseau, T. Open-framework inorganic materials. *Angew. Chem. Int. Edn* **38,** 3269–3292 (1999).
2. Yaghi, O. M., Li, H., Davis, C., Richardson, D. & Groy, T. L. Synthetic strategies, structure patterns, and emerging properties in the chemistry of modular porous solids. *Acc. Chem. Res.* **31,** 474–484 (1998).
3. Zaworotko, M. Nanoporous structures by design. *Angew. Chem. Int. Edn* **39,** 3052–3054 (2000).
4. Noro, S. I., Kitagawa, S., Kondo, M. & Seki, K. A new, methane adsorbent, porous coordination polymer [{CuSiF$_6$(4,4'-bipyridine)$_2$}$_n$]. *Angew. Chem. Int. Edn* **12,** 2081–2084 (2000).
5. Xu, X., Nieuwenhuyzen, M. & James, S. L. A nanoporous metal-organic framework based on bulky phosphane ligands. *Angew. Chem. Int. Edn* **41,** 764–767 (2002).
6. Bennett, M. V., Beauvais, L. G., Shores, M. P. & Long, J. R. Expanded prussian blue analogues incorporating [Re$_6$Se$_8$(CN)$_6$]$^{3-/4-}$ clusters: adjusting porosity via charge balance. *J. Am. Chem. Soc.* **123,** 8022–8032 (2001).
7. Pschirer, N. G., Ciurtin, D. M., Smith, M. D., Bunz, U. H. F. & zur Loye, H.-C. Noninterpenetrating square-grid coordination polymers with dimensions of 25×25 Å^2 prepared by using N,N'-type ligands: the first chiral square grid coordination polymer. *Angew. Chem. Int. Edn* **41,** 583–586 (2002).
8. Chen, B., Eddaoudi, M., Hyde, S. T., O'Keefe, M. & Yaghi, O. M. Interwoven metal-organic framework on a periodic minimal surface with extra-large pores. *Science* **291,** 1021–1023 (2001).
9. Barthelet, K., Marrot, J., Riou, D. & Férey, G. A breathing hybrid organic-inorganic solid with very large pores and high magnetic characteristics. *Angew. Chem. Int. Edn* **41,** 281–284 (2002).
10. Wynn, C. M., Albrecht, A. S., Landee, C. P., Turnbull, M. M. & Dodrill, B. Resonance in the nonlinear susceptibilities of Co$_3$BTCA$_2$(H$_2$O)$_4$, a molecular-based magnet. *J. Solid State Chem.* **159,** 379–384 (2001).
11. Forster, P. M. & Cheetham, A. K. Open-framework nickel succinate, [Ni$_7$(C$_4$H$_4$O$_4$)$_6$(OH)$_2$(H$_2$O)$_2$]·2H$_2$O: a new hybrid material with three dimensional Ni-O-Ni connectivity. *Angew. Chem. Int. Edn* **41,** 457–459 (2002).
12. Cotton, F. A., Lin, C. & Murillo, C. A. Supramolecular arrays based on dimetal building units. *Acc. Chem. Res.* **34,** 759–771 (2001).
13. Price, D. J., Tripp, S., Powell, A. K. & Wood, P. T. Hydrothermal synthesis, X-ray structure and complex magnetic behaviour of Ba$_4$(C$_2$O$_4$)Cl$_2$[{Fe(C$_2$O$_4$)(OH)}$_4$]. *Chem. Eur. J.* **7,** 200–208 (2001).
14. Chui, S. S.-Y., Lo, S. M.-F., Charmant, J. P. H., Orpen, A. G. & Williams, I. D. A chemically functionalizable nanoporous material [Cu$_3$(TMA)$_2$(H$_2$O)$_3$]$_n$. *Science* **283,** 1148–1150 (1999).
15. Moulton, B., Lu, J., Hajndl, R., Hariharan, S & Zaworotko, M. J. Crystal Engineering of a nanoscale Kagomé lattice. *Angew. Chem. Int. Edn* **41,** 2821–2824 (2002).
16. Kim, J. *et al.* Assembly of metal-organic frameworks from large organic and inorganic secondary building units: new examples and simplifying principles for complex structures. *J. Am. Chem. Soc.* **123,** 8329–8247 (2001).
17. Eddaoudi, M. *et al.* Systematic design of pore size and functionality in isoreticular MOFs and their application in methane storage. *Science* **295,** 469–472 (2002).
18. Beauvais, L. G. & Long, J. R. Co$_3$[Co(CN)$_5$]$_2$: A microporous magnet with ordering temperature of 38 K. *J. Am. Chem. Soc.* **124,** 12096–12097 (2002).
19. Laget, V., Hornick, C., Rabu, P., Drillon, M. & Ziessel, R. Molecular magnets hybrid organic-inorganic layered compounds with very long-range ferromagnetism. *Coordin. Chem. Rev.* **178,** 1533–1553 (1998).
20. Ballester, M. Inert free radicals: a unique trivalent carbon species. *Acc. Chem. Res.* **12,** 380 (1985).
21. Pech, R. & Pickardt, J. Catena-triaqua-μ-[1,3,5-benzenetricarboxylato(2-)]-copper(II). *Acta Cryst. C* **44,** 992–994 (1988).
22. Abourahma, H., Moulton, B., Kravtsov, V. & Zaworotko, M. J. Supramolecular isomerism in coordination compounds: nanoscale molecular hexagons and chains. *J. Am. Chem. Soc.* **124,** 9990–9991 (2002).
23. Min, K. S. & Suh, M. P. Self-assembly and selective guest binding of three-dimensional open-framework solids form a macrocyclic complex as a trifunctional metal building block. *Chem. Eur. J.* **7,** 303–313 (2001).
24. Lu, J. Y. & Babb, A. M. An extremely stable open-framework metal-organic polymer with expandable structure and selective adsorption capability. *Chem. Commun.* 1340–1341 (2002).
25. Kitagawa, S. *et al.* Novel flexible frameworks of porous (II) coordination polymers that show selective guest adsorption based on the switching of hydrogen-bond pairs of amide groups. *Chem. Eur. J.* **8,** 3587–3600 (2002).
26. Biradha, K. & Fujita, M. A springlike 3D-coordination network that shrinks or swells in a crystal-to-crystal manner upon guest removal or re-adsorption. *Angew. Chem. Int. Edn* **41,** 3392–3395 (2002).
27. Li, H., Davis, C. E., Groy, T. L., Kelley, D. G. & Yaghi, O. M. Coordinatively unsaturated metal centers in the extended porous framework of Zn$_3$(BDC)$_3$·6H$_2$O (BDC = 1,4-benzene dicarboxylate). *J. Am. Chem. Soc.* **120,** 2186–2187 (1998).
28. Maspoch, D., Ruiz-Molina, D., Wurst, K., Rovira, C. & Veciana, J. A very bulky carboxylic perchlorotriphenylmethyl radical as a novel ligand for transition metal complexes. A new spin frustrated metal system. *Chem. Commun.* 2958–2959 (2002).
29. Larionova, J., Mombelli, B., Sanchiz, J. & Kahn, O. Magnetic properties of the two-dimensional bimetallic compounds (NBu$_4$)[M^{II}Ru^{III}(ox)$_3$] (NBu$_4$ = Tetra-*n*-butylammonium; M = Mn, Fe, Cu; ox = oxalate). *Inorg. Chem.* **37,** 679–684 (1998).
30. Kahn, O. in *Molecular Magnetism* (ed. Kahn, O.) 251–332 (VCH, New York, 1993).
31. Caneschi, A., Gatteschi, D., Lalioti, N., Sangregorio, C. & Sessoli, R. Supramolecular interactions and magnetism of metal-radical chains. *J. Chem. Soc. Dalton Trans.* **2000,** 3907–3912 (2000).
32. Ivamura, H. & Inoue, K. in *Magnetism: Molecules to Materials* Vol. III (eds Miller, J. S. & Drillon, M.) 61–108 (Wiley-VCH, Weinheim, 2001).

Acknowledgements

This work was supported by the Programa Nacional de Materiales of the Dirección General de Investigación (Spain), under project MAGMOL. D.M. is grateful to the Generalitat de Catalunya for a predoctoral grant. We thank P. Gerbier of the Université Montpellier for TG-MS experiments and X. Alcobé of the Universitat de Barcelona for X-ray powder diffraction measurements.
Correspondence and requests for materials should be addressed to C.R or J.V.
Supplementary Information is available on the *Nature Materials* website (http://www.nature.com/naturematerials).

Competing financial interests

The authors declare that they have no competing financial interests.

Article I

Títol: EPR characterization of a nanoporous metal-organic framework exhibiting a bulk magnetic ordering.

Autors: D. Maspoch, J. Vidal-Gancedo, D. Ruiz-Molina, C. Rovira, J. Veciana.

Publicació: J. Phys. Chem. Solids, en premsa.

(No presentat a la Comissió de Doctorat)

ELSEVIER

Journal of Physics and Chemistry of Solids xx (2003) xxx–xxx

JOURNAL OF PHYSICS AND CHEMISTRY OF SOLIDS

www.elsevier.com/locate/jpcs

EPR characterization of a nanoporous metal-organic framework exhibiting a bulk magnetic ordering

D. Maspoch, J. Vidal-Gancedo, D. Ruiz-Molina, C. Rovira, J. Veciana*

Institut de Ciència de Materials de Barcelona, Campus UAB, Cerdanyola 08193, Spain

Received 27 June 2003; revised 14 August 2003

Abstract

Magnetic properties of the open-framework structure $[Cu_3(PTMTC)_2(py)_6(CH_3CH_2OH)_2(H_2O)]$ as well as those of a related evacuated sample have been analyzed on the basis of combined SQUID and EPR measurements. Such combined experiments demonstrate unambiguously the key role played by the radical ligand PTMTC in the promotion in both molecular magnets of magnetic exchange interactions through the open-framework structure.

Keywords: A. Metals; D. Elastic properties; D. Magnetic properties; D. Optical properties

1. Introduction

The use of chemical coordination techniques may allow the systematic design of open-framework structures with a considerable range of pore sizes and functionalities by using different organic ligands such as phosphane, cyano groups, N,N'-type ligands and polycarboxylic acids [1–4]. Furthermore, the use of transition metal ions opens the possibility to obtain nanoporous materials with additional electrical, optical or magnetic properties. Among them, the search for magnetic open-framework structures using polycarboxylic acids is a major challenge [5–10]. The interest is twofold. First, polycarboxylic acids have been proved to be good superexchange pathways for magnetic coupling and second, their use for the synthesis of open-framework structures may profit from crystal engineering techniques since they coordinate in a predictable way. For instance, Wood et al have described a new iron(II) oxalate structure with channels and a phase transition to an antiferromagnetic order state at 32 K [9]. On the other side, Williams et al. have described a new nanoporous metal coordination polymer using the 1,3,5-tricarboxylic acid, which exhibits a three-dimensional structure with a pore size of 1 nm and cooperative antiferromagnetic behavior [10].

Alternatively, enormous difficulties appear to expand pore sizes to diameters of 2 nm and beyond without compromising magnetic exchange interactions. Indeed, magnetic coupling between transition metal ions takes place through a superexchange mechanism involving ligand orbitals, mechanism that is strongly dependent on their relative orientation and specially, on the distance between interacting ions. Then, although Yaghi et al. have already described a systematic approach for the design of pore size and functionality based on the use of organic polycarboxylate ligands with different lengths and topologies [11,12]. such modifications are expected to decrease, or in the worst of the cases disrupt, the superexchange pathway.

In our group, we have developed a new synthetic strategy for the obtaining of metal-organic nanoporous materials with very large channels and strong magnetic exchange interactions based on the use of electronic open-shell organic ligands; i.e. organic free radicals as polydentate coordinating ligands [13]. The open-shell character of organic ligands is particularly appealing since they are expected to interact with transition metal ions enhancing the strength of magnetic interactions and the magnetic dimensionality of the nanoporous material in comparison with systems made up from paramagnetic metal ions and diamagnetic coordinating ligands.

For this synthetic approach we have chosen perchlorotriphenylmethyl (PTM) radical [14], which have its central

* Corresponding author. Tel.: +34-93-580-18-53; fax: +34-93-580-18-53.
E-mail address: vecianaj@icmab.es (J. Veciana).

0022-3697/$ - see front matter © 2003 Published by Elsevier Ltd.
doi:10.1016/j.jpcs.2003.11.026

carbon atom, where most of the unpaired electron is localized, sterically shielded by an encapsulation with six bulky chlorine atoms that increase its life expectancy and thermal and chemical stabilities. More precisely, we have used a persistent organic free radical functionalized with three carboxylic groups, the radical PTMTC. Using this approach, we have obtained the open-framework structure $[Cu_3(PTMTC)_2(py)_6(CH_3CH_2OH)_2(H_2O)]$, which we call MOROF-1, combining very large pores (2.8–3.1 nm) with a bulk magnetic ordering at low temperatures. In addition, MOROF-1 shows a reversible and highly selective solvent-induced 'shrinking-breathing' process involving large volume changes (25–35%) that strongly influence the magnetic properties of the material [13]. Removal of guest solvent molecules leads to an amorphous material (see Scheme 1), which even though exhibits a magnetic behavior related to that shown by crystals of MOROF-1 standing onto EtOH, although critical temperature is shifted down to 400 mK.

In this paper we report additional Electron Paramagnetic Resonance (EPR) studies to give more insight into the influence of the open-shell character of the ligand on the magnetic properties of MOROF-1. With this aim, EPR spectra from room temperature down to low temperatures of both, the crystalline material standing onto EtOH and the amorphous material, are reported. Finally, variable-temperature EPR spectra of MOOF-1, an open-framework isostructural to MOROF-1 where the radical ligand PTMTC has been replaced by its diamagnetic counterpart hydrocarbon, HPTMTC, is reported for comparison.

2. Experimental section

Compound MOROF-1 was prepared as previously described [13]. EPR spectra were obtained on a Bruker ESP-300E spectrometer operating at X-band (9.3 GHz), equipped with a rectangular cavity T102. Spectra were recorded in the 4–300 K range using a Bruker variable-temperature unit and an Oxford Instruments EPR-900 cryostat. The signal-to-noise ratio was increased by accumulation of scans using the F/F lock accessory Bruker ER 033M and a NMR gaussimeter Bruker ER 035M, to guarantee a high-field reproducibility. Precautions to avoid undesirable spectral line broadening such as that arising from microwave power saturation and magnetic field over-modulation were taken.

3. Results and discussion

The open-framework of as-synthesized crystals standing onto liquid EtOH of MOROF-1 consists of Cu^{2+}units with a square pyramidal coordination polyhedron composed by two monodentate carboxylic groups and two pyridine ligands (see Fig. 1). The remaining position on

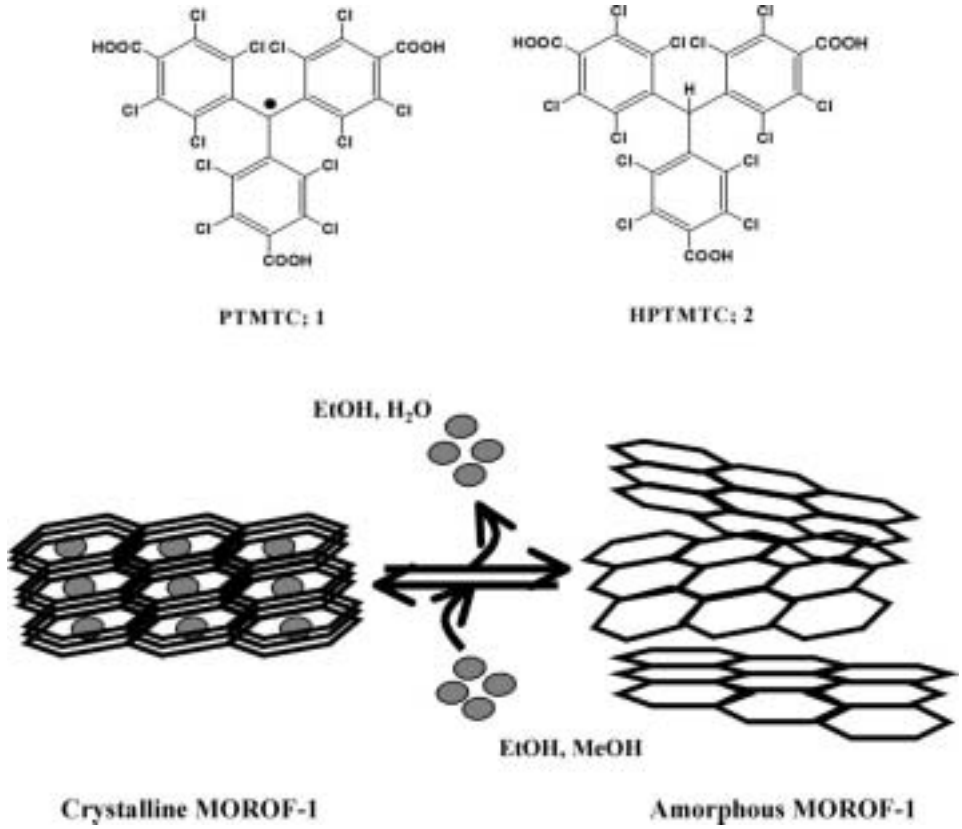

Scheme 1.

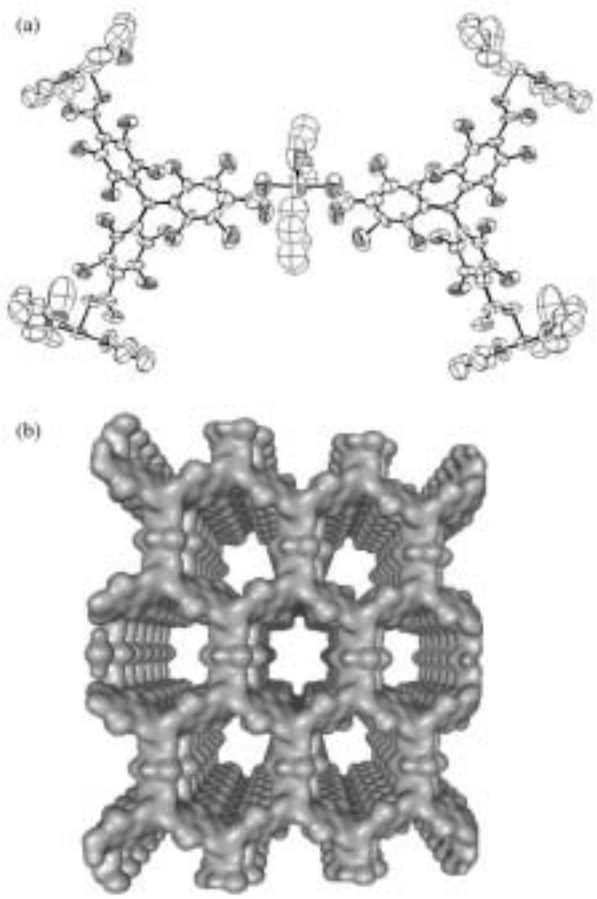

Fig. 1. Crystal structure of MOROF-1. (a) ORTEP plot of the building block. (b) Crystal packing of MOROF-1 showing the formation of hexagonal nanochannels along the *c* axes.

the coordination sites of metal centers is occupied by coordinative solvent molecules of ethanol or water. Thus, since each PTMTC is linked to three Cu(II) ions and each Cu(II) ion is bonded to two PTMTC radicals, a two-dimensional sheet is generated, extending along the ab plane with a honeycomb structure. Simultaneously, different layers pack between them forming an open-framework structure, generating a nanoporous architecture. Indeed, each hexagonal nanopores, composed of rings of six metal units and six PTMTC radicals, measure 3.1 and 2.8 nm between opposite vertices.

Magnetic properties shows a typical ferrimagnetic behavior, followed by a magnetic ordering at low temperatures (see Fig. 2). At room temperature, χT value is equal to 1.8 emu K mol^{-1}, a value that is in good agreement with that expected for non-interacting Cu(II) ions and PTMTC radicals, with a 3:2 stoichiometry and with local spins $S_{Cu} = S_{PTMTC} = 1/2$. The χT value decreases as the temperature is lowered, reaching a minimum value at 31 K that is a clear signature of the presence of strong antiferromagnetic couplings between $Cu^{2+}$and $PTMTC^{3-}$ ions within the honeycomb layers. As temperature is further decreased, the χT curve increases very rapidly up to a maximum value around 2 K, which can be explained by an increase of the correlation length of antiferromagnetic coupled units as randomising thermal effects are reduced, either via in-plane long-range antiferromagnetic coupling or interplane ferromagnetic interactions.

EPR experiments were carried out over the temperature range of 4–300 K in the presence of mother liquor to avoid the loss of solvate guess molecules. Selected spectra at four different temperatures (5, 60, 156 and 300 K) are shown in Fig. 3. The EPR spectrum at room temperature exhibits two broad lines, showing distinct intensities that are tentatively assigned to solid MOROF-1, and a third narrow line attributed to the presence of a small amount of free PTMTC present in the mother liquor. Indeed, such a narrow line is centered at $g = 2.0020$ and exhibits a linewidth of 0.1–0.2 mT, characteristic of a substituted PTM radicals [15]. On the other side, the two main lines centered at $g = 2.3227$ and $g = 2.0883$ coming from MOROF-1 exhibit linewidths of 8 and 19 mT, respectively, and different intensities. Such characteristic signals are not originated by individual contributions from the Cu(II) and/or the organic radicals (vide infra) but are the result of the interaction between the two types of spin centers. Such interactions are rather complicated and have not been investigated before. To give more details into these signals, variable-temperature spectra were recorded. On decreasing the temperature, the intensity of the main signal centered at higher field increases whereas the weaker satellite line observed at a lower field gradually decreases until approximately 60 K, temperature at which it completely disappears. A further decrease of the temperature below 50 K shows the transformation of the remaining line, into a broader signal with a more complex pattern. Such a complex pattern is assigned to the development of regions with different correlation length of antiferromagnetically coupled Cu(II) ions and $PTMTC^{3-}$ organic radicals, since we are getting closer to the ordering temperature of MOROF-1, as previously confirmed by solid-state magnetic SQUID measurements.

In addition to the considerable variable-temperature dependence of the shape and intensity of the line, another important feature that deserves to be mentioned is the strong temperature dependence of the *g*-value [16]. The shift of the *g* value of the band appearing at higher field with the temperature from room temperature down to 4 K is shown in Fig. 4. As can be seen there, from room temperature down to approximately 90 K the *g* value remains practically constant. Below 90 K, the *g* value starts to increase gradually at the beginning and more steeply at lower temperatures, as the critical temperature is reached, up to a value of 2.2551 at 5 K. Once the presence of possible phase-transitions at low temperatures has been ruled out, this notable shift in the *g* factor is due to the effect of the strong internal magnetic field developed because of the magnetic ordering of the sample. This internal magnetic field at 5 K may be estimated as 24.3 mT.

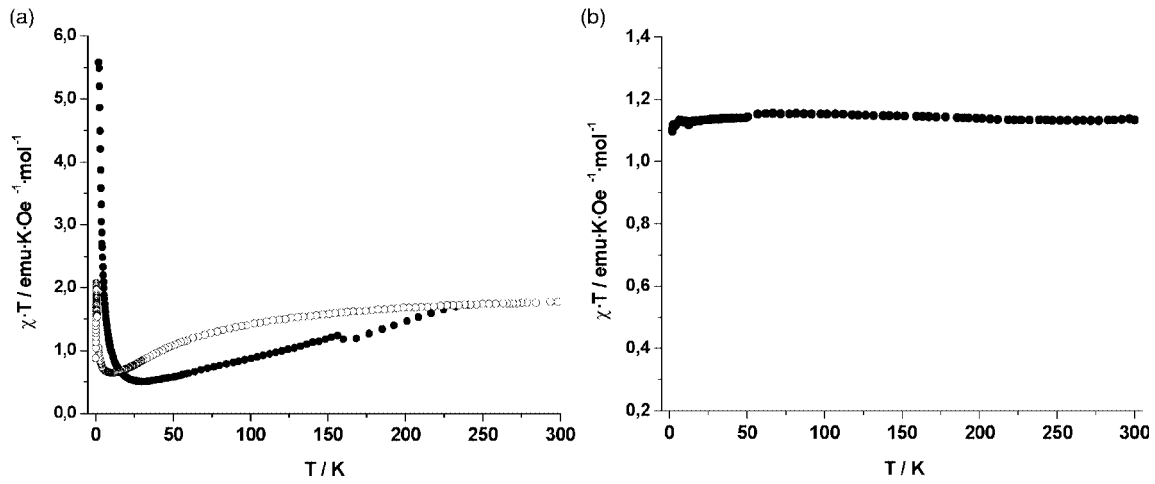

Fig. 2. Magnetic measurements. (a) Value of χT as a function of the temperature for MOROF-1 (● as-synthesized MOROF-1, o evacuated MOROF-1). (b) Value of χT as a function of the temperature for MOOF-1.

Once the as-synthesized crystals standing onto EtOH of MOROF-1 were investigated, we focused our attention in an evacuated sample of MOROF-1, which, as described at the introduction, is amorphous. First, SQUID measurements indicate a similar magnetic behavior in comparison with the as-synthesized crystals standing onto mother liquor (see Fig. 2). Indeed, at room temperature, χT value is equal to 1.8 emu K mol^{-1}, a value that is in good agreement with that expected for non-interacting Cu(II) ions and PTMTC radicals, with a 3:2 stoichiometry and with local spins $S_{Cu} = S_{PTMTC} = 1/2$. Then, the χT value decreases as the temperature is lowered, reaching a minimum value at 11 K whereupon it increases very rapidly up to a maximum value around 400 mK. The main difference with the magnetic properties of an as-synthesized sample of MOROF-1 relies in the position of the minimum and maximum values. From these results, it can be inferred that the effective strength of the magnetic exchange interactions between the Cu(II) and PTMTC radical units decreases for the evacuated sample.

EPR measurements of an evacuated sample of MOROF-1 were carried out over the temperature range of 4–300 K. Selected spectra at four different temperatures (5, 60, 140 and 300 K) are shown for comparison purposes in Fig. 5. At room temperature a single broad line was observed at $g = 2.0887$ with a linewidth of 19 mT. Such values are similar to those previously found for as-synthesized crystals of MOROF-1, with the main difference relying on the lack of the weaker satellite line observed at a lower field. A decrease of the temperature reveals minor changes. Only at very low temperatures, c.a. 5 K, a structured signal with a poor resolution appears. Moreover, variations of the g value with temperature were recorded from room temperature down to 4 K (see Fig. 4). As can be seen there, from room temperature down to approximately 45 K, that the g value remains practically constant. Below 45 K, the g value starts to increase gradually at the beginning and more steeply at lower temperatures up achieving a value of 2.1798 at 5 K. The latter value and the temperature at which the g-value starts to increase, are considerable smaller than those

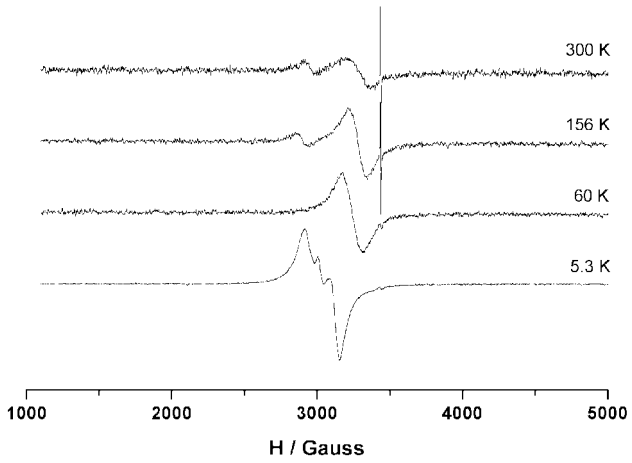

Fig. 3. ESR spectrum of a microcrystalline sample of as-synthesized MOROF-1 in ethanol solution at 300, 156, 60 and 5.3 K.

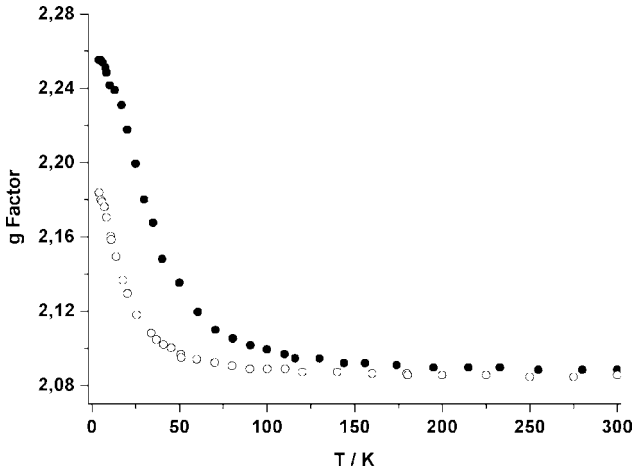

Fig. 4. Temperature dependence of the experimental g-factor observed for (●) as-synthesized MOROF-1 and (o) amorphous MOROF-1.

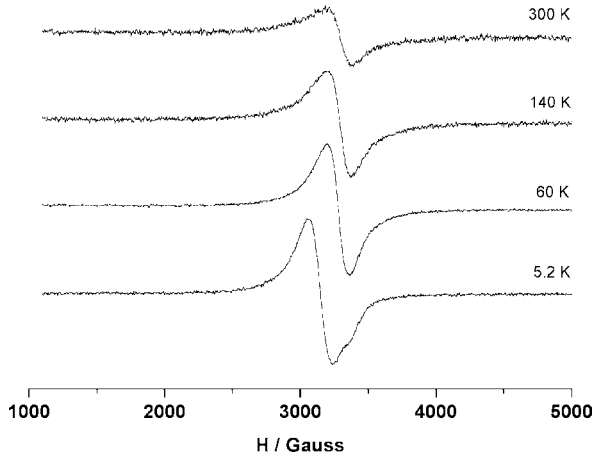

Fig. 5. ESR spectrum of amorphous MOROF-1 at 300, 140, 60 and 5.2 K.

found for an as-synthesized sample of MOROF-1. This fact indicates that the internal magnetic field developed is lower than in the crystalline sample, a result which is in agreement with a decrease of the effective magnetic exchange interactions, as observed by SQUID measurements.

Finally, the magnetic properties of MOOF-1, a metal–organic open-framework complex, isostructural to MOROF-1 in which the radical ligand PTMTC has been replaced by its diamagnetic counterpart hydrocarbon HPTMTC, have been studied. SQUID magnetic measurements of a microcrystalline sample MOOF-1 in the presence of mother liquor show a quasi-ideal paramagnetic behavior in the whole range of studied temperatures; i.e. from room temperature down to 2 K (see Fig. 2). The effective magnetic moment in the whole temperature range is in agreement with the presence of non-interacting isolated Cu(II) ions ($S = 1/2$ centers). These results were supported by EPR experiments. The EPR spectrum of MOOF-1 at room temperature in the presence of mother liquor is shown in Fig. 6 along with those of MOROF-1 and a related evacuated sample for comparison purposes. As can be seen in this figure, at room temperature MOOF-1 exhibits a unique asymmetric line centered at $g = 2.0805$, characteristic of the paramagnetic Cu(II) ion with a low magnetic anisotropy. Moreover, on decreasing the temperature no change either of the g-value nor the shape of the signal was detected. The only significant change was the increase of its intensity on decreasing the temperature, according with the Curie law, as expected for a paramagnetic species. These results demonstrate clearly the magnetic isolation of Cu(II) ions in MOOF-1 showing the key role played by the radical ligands in MOROF-1 in transmitting the magnetic exchange interactions through the open-framework structure.

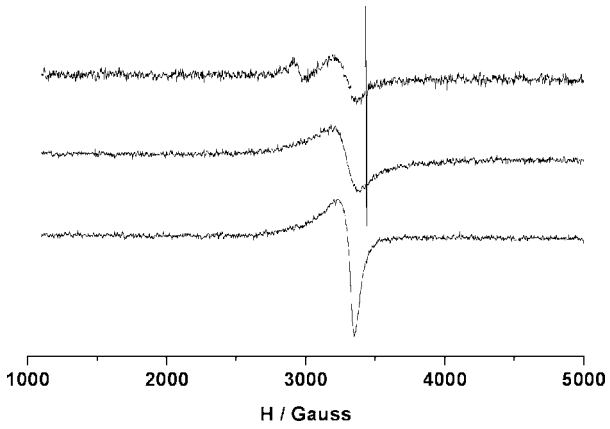

Fig. 6. ESR spectrum at room temperature of the as-synthesized MOROF-1 (top), amorphous MOROF-1 (medium) and MOOF-1 (bottom).

4. Conclusions

The magnetic properties of the open-framework structure MOROF-1, as well as those of a related evacuated sample, have been analyzed on the basis of combined SQUID and EPR measurements. The results confirm that even though the bulk magnetic ordering shown by MOROF-1 is retained after its ‘shrinking’ process, although removal of guest solvent molecules leads to the obtaining of an amorphous material with smaller magnetic exchange interactions, and therefore, with a critical temperature shifted to a lower value. Moreover, the key role played by the radical ligand PTMTC to promote magnetic exchange interactions through the open-framework structure of MOROF-1 have also been demonstrated.

Acknowledgements

This work was supported from DGI (project MAT 2000-1388-C03-01), CIRIT (project 2000 SGR 00114)) and the 3MD Network of the TMR program of the E.U. (contract ERBFMRXCT 980181). D.M. thanks the Generalitat de Catalunya for a predoctoral grant. D.M. is enrolled to the PhD program of the Universitat Autonoma de Barcelona.

References

[1] X. Xu, M. Nieuwenhuyzen, S.L. James, Angew. Chem. Int. Ed. 41 (2002) 764–767.
[2] M.V. Bennett, L.G. Beauvais, M.P. Shores, J.R.J. Long, J. Am. Chem. Soc. 123 (2001) 8022–8032.
[3] N.G. Pschirer, D.M Ciurtin, M.D. Bunz, U.H.F. zur Loye, H.-C. Angew, Angew. Chem. Int. Ed. 41 (2002) 583–586.
[4] B. Chen, M. Eddaoudi, S.T. Hyde, M. O’Keefe, O.M. Yaghi, Science 291 (2001) 1021–1023.
[5] K. Barthelet, J. Marrot, D. Riou, G. Férey, Angew. Chem. Int. Ed. 41 (2002) 281–284.
[6] C.M. Wynn, A.S. Albrecht, C.P. Landee, M.M. Turnbull, B.J. Dodrill, Solid State Chem. 159 (2001) 379–384.
[7] P.M. Forster, A.K. Cheetham, Angew. Chem. Int. Ed. 41 (2002) 457–459.
[8] F.A. Cotton, C. Lin, C. Murillo, Acc. Chem. Res. 34 (2001) 759–771.

[9] D.J. Price, S. Tripp, A.K. Powell, P.T. Wood, Chem. Eur. J. 7 (2001) 200–208.
[10] S.S.Y. Chui, S.M.F. Lo, J.P.H. Charmant, A.G. Orpen, I.D. Williams, Science 283 (1999) 1148–1150.
[11] J. Kim, B. Chen, T.M. Reineke, H. Li, M. Eddaoudi, D.B. Moler, M. O'Keefe, O.M. Yaghi, J. Am. Chem. Soc. 123 (2001) 8239–8247.
[12] M. Eddaoudi, J. Kim, N. Rosi, D. Vodak, J. Wachter, M. O'Keefe, O.M. Yaghi, Science 295 (2002) 469–472.
[13] D. Maspoch, D. Ruiz-Molina, K. Wurst, N. Domingo, M. Cavallini, F. Biscarini, J. Tejada, C. Rovira, J. Veciana, Nature Mat. 2 (2003) 190.
[14] M. Ballester, Acc. Chem. Res. 12 (1985) 380.
[15] O. Armet, J. Veciana, C. Roviera, J. Riera, J. Castañar, E. Molins, J. Rius, C. Miravitlles, S. Olivella, J. Brichfeus, J. Phys. Chem. 91 (1997) 5608.
[16] A. Bencini, D. Gatteschi, EPR of exchange coupled systems, Springer, 1990.